Polar Geosci 15, 112-122, 2002

Detection of grounding line and vertical displacement of ice shelf by SAR interferometry — A case study for the Stanjukovicha Ice Shelf, East Antarctica, using ERS tandem SAR data —

Taku Ozawa*, Kazuo Shibuya, Koichiro Doi and Shigeru Aoki

National Institute of Polar Research, Kaga 1-chome, Itabashi-ku, Tokyo 173-8515

Abstract: Synthetic Aperture Radar (SAR) interferometry was applied to the Stanjukovicha Ice Shelf, East Antarctica, to detect its grounding lines and vertical motion and to monitor the ice shelf behavior. The ERS-1 and -2 tandem mission data were used. Fringes were clearly revealed on the obtained interferograms. By tracing the inland side of the dense fringes, the grounding lines were obtained not only for the boundary between the continental ice sheet and the ice shelf, but also for the boundaries around the small "islands". The grounding lines derived from SAR interferometry were not always accompanied by clear changes in surface properties of SAR intensity images. Since the displacement fringes include the component of horizontal ice flow, the component of vertical displacement was extracted by counting only the phase difference along the ice flow lines not absolute phase difference. The derived vertical displacements agreed well with modeled sea surface height changes with a standard deviation of 4.9 cm. Thus, the SAR interferometry demonstrated its ability and applicability in monitoring the Antarctic ice shelf.

key words SAR interferometry, Stanjukovicha Ice Shelf, ocean tide grounding line, ERS tandem mission

1. Introduction

Ice shelf-ocean margins around Antarctica are crucial areas in studying the global freshwater cycle. However, there are many logistic difficulties in conducting *in situ* geodetic surveys in these areas. The locations of grounding lines, which are the boundaries between the ice shelf and the area where the ice sheet grounds on the bedrock, are important variables in monitoring the stability of the ice shelf and ice mass flux. Many studies have been attempted to detect them by a remote sensing technique based on ice surface roughness changes across the grounding lines (*e.g.*, Orheim, 1978; Kim *et al.*, 2001). However, little is known about the basic relationship between surface roughness properties and underlying ground conditions, and the spatial resolution of applied images is not sufficient in many cases. Thus it would be helpful to use a geodetic remote sensing

*Present address: Japan Society for the Promotion of Science/Geographical Survey Institute, 1 Kitasato, Ibaraki 305-0811.

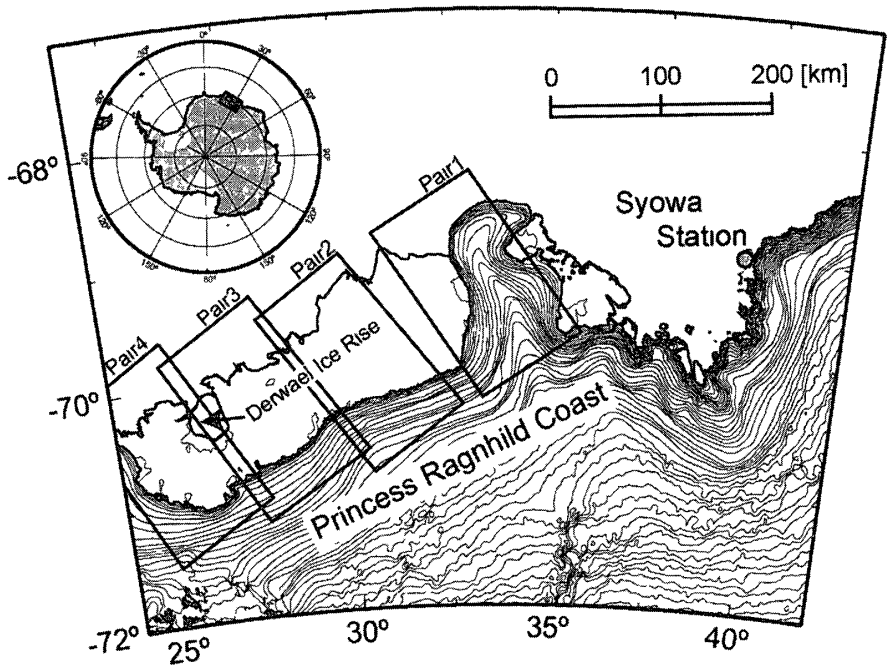

Fig 1 Map around Stanjukovicha Ice Shelf Solid boxes indicate SAR scene areas of Pairs 1 to 4 Coastlines and topographic contours are depicted using the Antarctic Digital Database (ADD British Antarctic Survey, 1998) Solid circle indicates the location of Syowa Station (39 5°E, 69 0°S)

technique with improved accuracy

Ocean tide observations in the marginal seas around Antarctica also have logistic difficulties Recently, ocean tide models have been greatly improved with the development of satellite altimetry (*e g.*, Matsumoto *et al* , 1995, 2000) However, the accuracies of the models are not known in the marginal areas around Antarctica, because of the sparseness of *in situ* observations and inherent difficulties in satellite altimetry Therefore, further independent observations are needed for the improvement of ocean tide models, a geodetic remote sensing technique would be useful for such an objective

Goldstein *et al* (1993) applied ERS-1 Synthetic Aperture Radar (SAR) interferometry, which is one of the geodetic remote sensing techniques, to the Rutford Ice Stream, West Antarctica, and showed the usefulness of SAR interferometry in monitoring the ice flow and the grounding line Rignot (1996) applied ERS-1 SAR interferometry to Petermann Gletscher, Greenland, and proposed a method which is able to measure the location of the grounding line and the vertical displacement of the ice tongue caused by the ocean tide This method, however, needs more than two interferograms acquired on the same satellite track Furthermore it also needs Digital Elevation Model (DEM), and thus the applicable areas are limited Moreover, this method can measure only the difference between the vertical displacements measured from the first and second interferograms

Ozawa *et al* (1999) applied ERS-1 SAR interferometry to the Zubchatyy Ice Shelf area, East Antarctica, and detected grounding lines and vertical displacement of the ice shelf by a simple method This method detects those from one interferogram with the

Table 1 Summary of SAR data

1	2	3	4	5
1	1996/4/2	4/3	27 5	361 5
2	1996/4/11	4/12	70 3	141 4
3	1996/4/17	4/18	15 5	641 9
4	1996/5/28	5/29	61 4	161 9

Column 1 Interferometric pair number
Column 2 Acquisition date of ERS-1
Column 3 Acquisition date of ERS-2
Column 4 Perpendicular component of baseline in meter
Column 5 Topographic height change per 1 cycle phase change in meter

assumption that the horizontal movement of the ice shelf is negligible They showed that the obtained vertical displacement was in good agreement with the modeled one using the ORI96 ocean tide model (Matsumoto *et al*, 1995) This method is not more accurate than the method by Rignot (1996), but is useful in a region where a DEM is not available and where there are few SAR data, and the absolute vertical displacement of the ice shelf can be measured However, there were still some problems to be solved in this method Generally, the effect of horizontal movement of ice shelves cannot be neglected There were no appropriate principles in selecting the point pairs from which their vertical displacements were calculated

In this study, we apply SAR interferometry to improve the detection of the grounding lines and extend the applicable areas in deriving the vertical displacement of ice shelves Another objective is to extend the analysis domain to much broader areas in our ongoing project of mapping and monitoring over East Antarctica The study area is the Stanjukovicha Ice Shelf (Fig 1) located along the Princess Ragnhild Coast and about 250 to 550 km west of Syowa Station (39 5°E, 69 0°S) The width of this ice shelf is about 100 km in the latitudinal direction and about 300 km in the longitudinal direction This area is one of the intensive observation areas of Japanese Antarctic Research Expeditions (JARE), and operations have been conducted to map the coast lines, ice shelf margin, topographic elevation and so on Thus the area is suitable for the establishment of the new technique and for monitoring its behavior continuously

2. SAR data and interferograms

SAR data used in this study were obtained by ERS-1 and ERS-2 satellites operated by the European Space Agency These satellites were designed with the same specifications, and ERS-2 passed through the same orbit as ERS-1 one day later These tandem SAR data pairs have an advantage for SAR interferometry, because the temporal decorrelation is low as mentioned by Zebker and Villasenor (1992) The ERS-1 and -2 tandem SAR data were intensively acquired from February 15 through June 3, 1996, at Syowa Station (Doi *et al*, 1999) We selected four tandem SAR data pairs observed around Stanjukovicha Ice Shelf (Table 1) These data were converted to level 0 CEOS format, which is applicable to various SAR processors (Doi *et al*, 2000) We generated the single look complex (SLC) images and SAR interferograms for each pair (Fig 2)

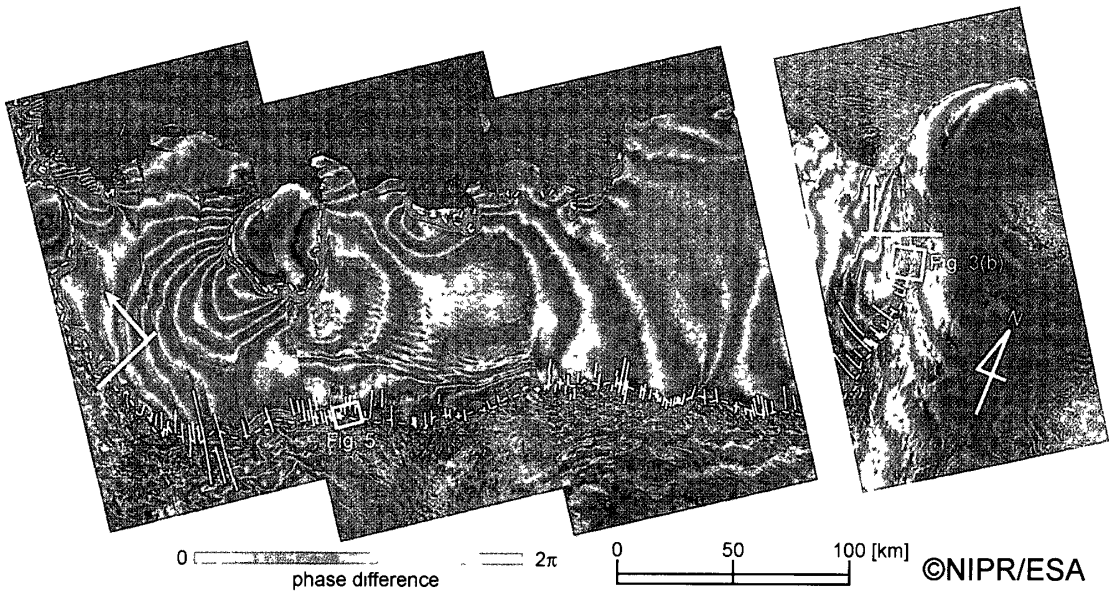

Fig 2 Mosaicked interferograms superposed on SAR intensity image The color bar indicates the phase from $-\pi$ to $+\pi$ Dashed white curves are the grounding lines obtained by SAR interferometry White lines show the representative ice flow lines from the SAR intensity image Yellow arrows show the area not used in calculation of vertical displacement The white boxes indicate the areas in Fig 3b and Fig 5

The coherences of the obtained SAR interferograms were very good and clear fringes appeared except in part of Pair 2 Decorrelation in Pair 2 may be caused by its long baseline (see Table 1) and/or scattering change on the ice shelf surface, as mentioned by Zebker and Villasenor (1992) Fortunately, however, we can count fringes of grounding lines, because the decorrelation appeared only in the central area of the ice shelf These interferograms were flattened using the precise ephemeris and ground control points (GCPs) The phase on an interferogram consists of both the topographic phase caused by topographic features and the displacement phase caused by horizontal ice flow and/or vertical displacement due to oceanic changes On the ice shelf, we can assume that the phase is only due to the displacement phase, because the surface of the ice shelf is sufficiently "flat" in estimating the topographic phase effect The elevation of the grounding line on the surface was estimated as less than 200 m from the 1 5,000,000 scaled map of East Queen Maud Land-Enderby Land (National Institute of Polar Research, 1988), and then the topographic phase will be 0 3 to 1 4 cycles or less on the ice shelf for the each pair If it is assumed that the surface elevation decreases linearly in the zone about 100 km from the grounding line (<200 m) to the margin of the ice shelf on the sea surface (0 m), the topographic fringes will be 0 03 to 0 14 cycles in a 10 km width This amount is comparable to only 1 to 4 mm of displacement in the line-of-sight (LOS) direction, which is the illuminating direction of radar Oceanic height variations are usually an order or two larger on the time scales of the tandem data acquisitions, and thus the displacement fringe will be the dominant component on the shelf in the generated interferograms

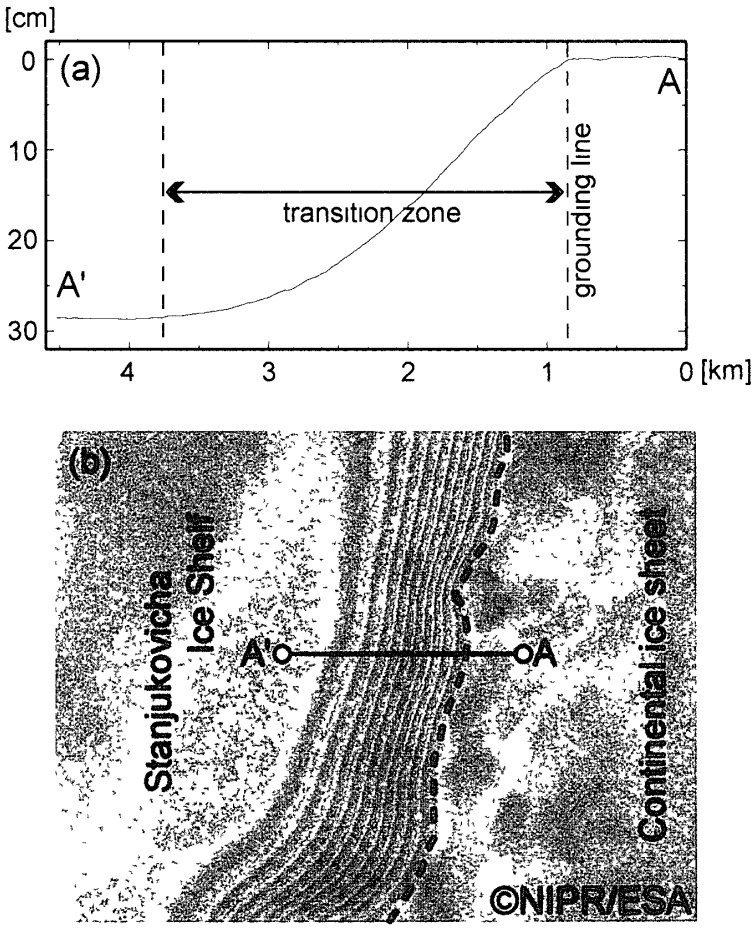

Fig 3 (a) Vertical displacement profile along A-A' line Dashed lines indicate the bending area due to ocean tide (called 'transition zone' in this paper) (b) Enlarged interferogram for the white box in Fig 2 Dashed curve indicates the obtained grounding line The points A and A' are shown with circles

3. Detection of the grounding lines

The grounding line is the boundary between ice grounded on the bedrock and ice floating on the seawater The ice shelf on the water moves vertically with sea surface height change caused by oceanic processes, whereas the grounded portion is not affected by the processes Part of the ice shelf near the grounding line (called the "transition zone" in this paper) is bent in a width of several kilometers taking the grounding line as a supporting point (the displacement profile shows in Fig 3a) Therefore dense fringes appear in the transition zone (Fig 3), because the positions of the displacement fringes are equal to those of co-displacement contour lines Then we can precisely detect the grounding line by tracing the grounded area boundary of the dense fringes (the broken line in Fig 3b) The accuracies in position of the derived grounding lines must be within 20 pixels (about 600 m) for Pairs 1, 3 and 4, because dense fringes clearly appear in the transition zones Unfortunately the dense fringes did not appear for Pair 2 The reason must be that the bending in the transition zone was actually small, because the sea surface height change for this pair was expected to be small at that time from an ocean tide model

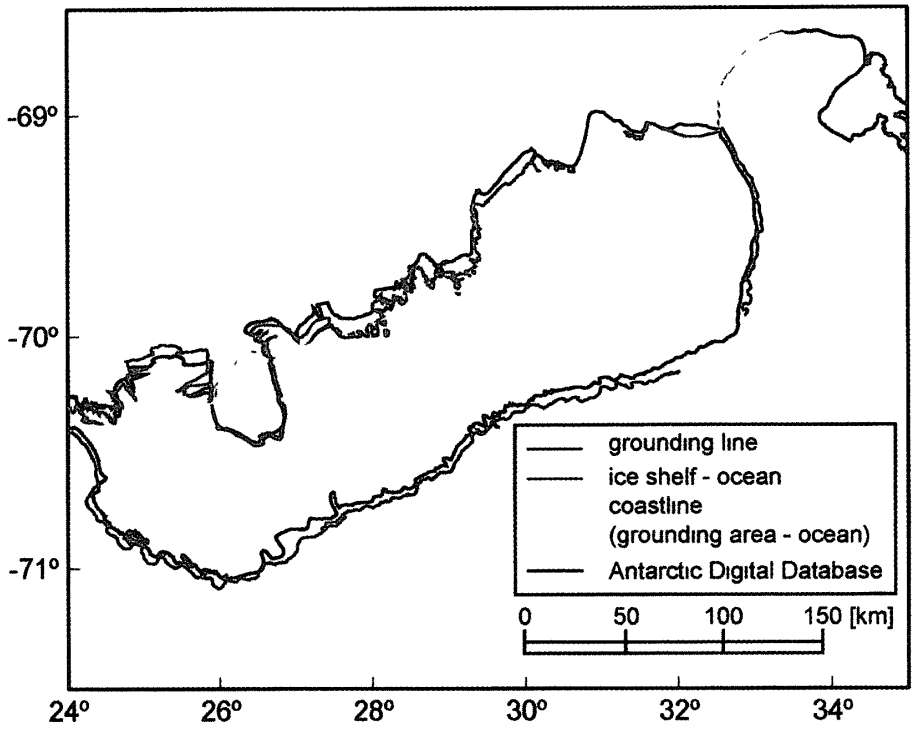

Fig 4 Comparison between the obtained grounding line and that of the Antarctic Digital Database (ADD British Antarctic Survey, 1998) Colored lines are determined by SAR Blue, red and yellow curves are the obtained grounding line by SAR interferometry, marginal line of ice shelf and coastline (grounding area-ocean boundary), respectively Solid curves indicate those from ADD

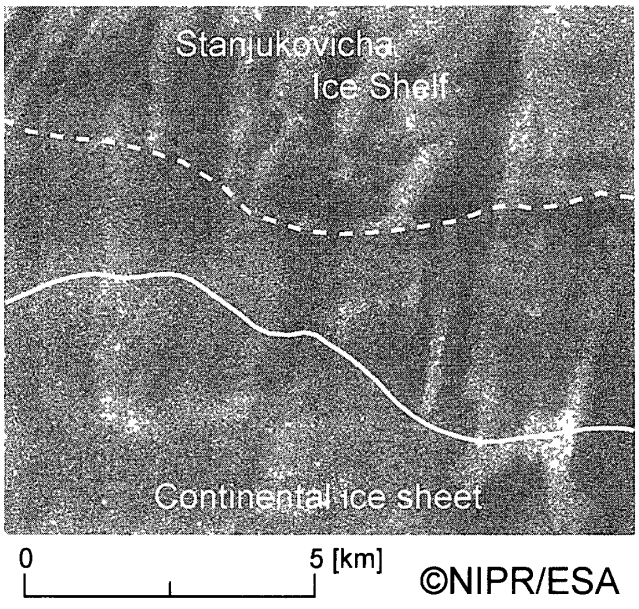

Fig 5 Comparison between grounding line derived from SAR interferometry (white curve) and that from SAR intensity image (dashed curve) The SAR intensity image area is consistent with the white box in Fig 2

Thus the accuracy of the grounding line detection for Pair 2 was lower than that for the other pairs

The obtained grounding lines (broken white lines in Fig 2) were not only the boundaries between the ice shelf and the continental ice sheet areas, but also those around small "islands" (the word is used hereafter, although we do not know their actual ground structures) For example, the grounding lines can be clearly identified around Derwael Ice Rise and the small islands east of it It was difficult to discriminate these small islands using usual satellite imagery sensors or even by aerial photography The applicability for unmapped islands is one of the advantages of SAR interferometry

GCPs are generally needed for constraining the obtained grounding line to geographic coordinates However, no GCPs were available on the SAR images used here As a compromise we use the coastlines from the Antarctic Digital Database (ADD British Antarctic Survey, 1998) as GCPs, the conversion parameters were determined so that the coastlines obtained from the SAR images (grounding area-ocean yellow lines in Fig 4) are adjusted to those of ADD by eye

Comparing the obtained ice sheet-shelf grounding lines (blue lines in Fig 4) with those of ADD (solid lines in Fig 4), the obtained grounding lines were generally located several kilometers inland of those of ADD Though the ADD data were mainly based on satellite optical images, we suspect that this difference is caused by the inaccuracy of discriminating grounding lines from those images It seems that the grounding lines obtained from SAR intensity images are located around the same or offshore area of those of ADD (Fig 5 of Kim *et al*, 2001) This suggested that the grounding lines obtained from the SAR intensity image were mostly equal to those from the optical image Comparing the grounding lines obtained from SAR interferometry with the SAR intensity image in this study (Fig 5), it seems that those derived from the SAR intensity image were located offshore of those from the SAR interferometry This suggests that the surface feature change on the ice shelf does not always coincide with the grounding line Thus, to detect the grounding line within 1 km accuracy, SAR interferometry is the probable technique which can provide physically proper evidence

4. Detection of the vertical displacement

4 1 Detection of sea surface height change caused by ocean tides and its error estimation

The ice shelf surface moves vertically with a sea surface height change by oceanic processes including tides, with thinning due to basal melting, and so on If the vertical displacement is to be measured by SAR interferometry, that is mainly due to the sea surface height change on time scales of several days or shorter However, the vertical displacement cannot be directly derived from the absolute phase, because the phase obtained from SAR interferometry also includes the component of horizontal ice flow

To cancel or reduce the horizontal motion, special care was taken in counting the phase differences If the ice flow speed is the same along the flow direction within the transition zone (*e g*, the zone between A and A′ in Fig 3), the contribution of the horizontal ice flow component is common for the two points Then the phase difference on each side of the transition zone is considered to be the vertical displacement component

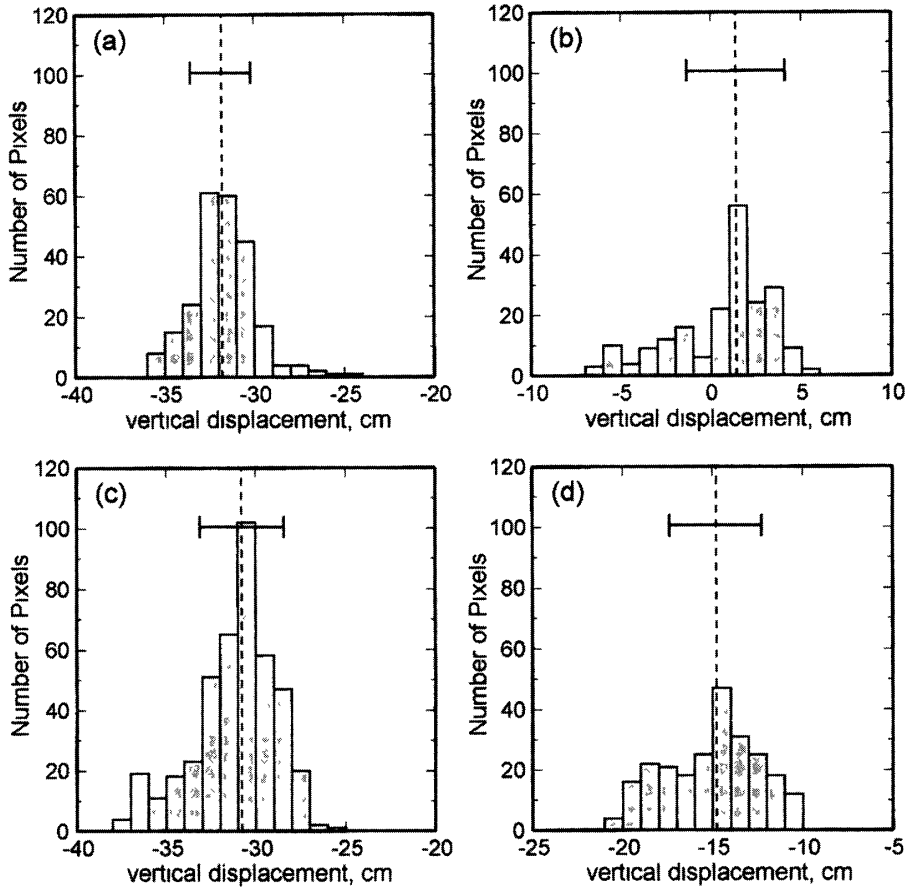

Fig 6 Histograms of the obtained vertical displacement Figure a to d are for Pairs 1 to 4, respectively Dashed lines show the median values Bars show the standard error calculated from the root-mean-square of residuals

We calculated the phase difference between a point on the inland side of the grounding line (10 pixels (about 200 m) from the grounding line) and one on the offshore side (400 pixels (less than 10 km) off) It is assumed that the flow direction is consistent with the direction perpendicular to the grounding line This assumption is considered to be reasonable from the actual SAR data, if the flow lines appeared on the SAR intensity images (representative flow lines are shown by white lines in Fig 2) are equal to the actual flow directions, the flow directions were in good agreement with the direction perpendicular to the grounding lines derived from SAR interferometry However, the areas around the east and west ends of the ice shelf (yellow arrows in Fig 2) were not used in this calculation, because this assumption may not be applicable to these areas Figure 6a to 6d show the histograms of the obtained vertical displacements calculated from the LOS component by taking the incidence angle to be 23 5° for Pairs 1 to 4, respectively, and the vertical displacement for each pair was derived from their median value (broken lines in Fig 6 and Table 2) Their errors, estimated from the root-mean-square of residuals, were 1 7 to 2 7 cm (bars in Fig 6 and Table 2) This error is probably due to spatial variations in speed of horizontal motion, uncertainty in the derived flow lines, and random noise on the SAR interferograms

In addition to the above errors, the error factors in SAR interferometry are generally

Table 2 Comparison of sea surface height changes between SAR interferometry results and modeled ones

1	2	3	4	5	6	7	8
1	−31 8	1 7	−20 2	−11 6	−9 8	−1 8	242
2	1 4	2 7	7 2	−5 8	−13 1	7 3	202
3	−30 8	2 3	−12 1	−18 7	−12 6	−6 1	421
4	−14 8	2 5	−16 3	1 5	0 7	0 8	239

Column 1 Interferometric pair number
Column 2 Obtained vertical displacement from SAR interferometry in centimeters A positive value indicates that sea surface height rises
Column 3 Standard error for obtained vertical displacement in centimeters
Column 4 Sea surface height change calculated from ORI96 ocean tide model in centimeters
Column 5 Difference between InSAR results and ORI96 results in centimeters
Column 6 Inverse barometers calcurated from NCEP re-analysis atmospheric pressure in centimeters
Column 7 Difference between InSAR results and model results is considered an inverse barometer (column 5+column 6) in centimeters
Column 8 Number of pixels in calculation of InSAR results

expected to be 1) the incompleteness in removing orbital and topographic fringes and 2) the tropospheric delay 1) In the present study, however, the error caused by the incompleteness in removing the orbital and topographic fringes is small, because the ice shelf is approximately flat and the distance between the two points (*e g*, A and A′ in Fig 3) is short 2) The error caused by tropospheric delay should also be small, because the water vapor in the atmosphere of low air temperature is few The total error caused by these factors will be less than 0 5 cycles, this amounts to an error of about 1 5 cm in the vertical displacement Taking this into account, the total error for the final vertical displacement observed with this method should be 2 3 to 3 1 cm

4 2 Comparisons between the obtained and modeled sea surface height changes

To evaluate the obtained vertical displacements, we compared them with the modeled estimates using the ORI96 ocean tide model (Matsumoto *et al*, 1995) The differences between the obtained and modeled vertical displacements were 1 5 to 18 7 cm, and the standard deviation for four pairs was 7 4 cm (Table 2) However, the actual sea surface height change varies with atmospheric pressure (*i e*, the inverse barometer effect) Direct observations of atmospheric pressure were not available in this analysis region, so we used sea level pressure data of the National Centers for Environmental Prediction (NCEP) reanalysis to estimate the inverse barometer effect Taking the barometric effect into account, differences were reduced to 0 8 to 7 3 cm (Table 2), and the standard deviation was reduced to 4 9 cm Especially, the obtained sea surface height changes of Pairs 1 and 4 were in good agreement with the modeled ones within 2 cm discrepancies, but the differences in Pairs 2 and 3 were around 6 to 7 cm, which were larger than the derived

intrinsic accuracy of 3 1 cm of the SAR interferometry The observation periods of the ERS-1/-2 SAR data for Pairs 2 and 3 coincided well with the times of large atmospheric pressure variations Those sudden changes in atmospheric pressure cannot be fully resolved in the NCEP reanalysis data If these differences were caused by the atmospheric effect, SAR interferometry may contribute to the validation of atmospheric models with accurate ocean tide models

5. Summary and conclusions

The grounding lines of Stanjukovicha Ice Shelf were detected using SAR interferometry of the ERS-1/-2 tandem mission, taking ice shelf dynamics into account The locations of the derived grounding lines suggested an interesting problem in comparing various techniques and data sets for the detection of the grounding lines We found that there was a case in which the grounding lines derived from the SAR intensity images were located to the offshore side of the actual location, and SAR interferometry is a useful technique for detection of the accurate location of the grounding lines It was demonstrated that SAR interferometry is also effective in detecting ice islands in unmapped regions

We also calculated the sea surface height change by adopting two points situated on opposite sides of the transition zone The horizontal ice flow component is canceled or reduced by counting the phase difference between the two points The derived vertical displacements agreed well with modeled sea surface height changes, which include the barometric effect This result shows that this method can measure the sea surface height change accurately from one interferogram Such SAR interferometry will become a useful technique in validating ocean tide models in marginal waters around Antarctica Thus it was demonstrated that SAR interferometry is one of the key techniques for continuous monitoring of Antarctic ice shelf areas

Acknowledgments

Dr K Moriwaki substantially contributed to revision of nomenclature, and provided invaluable information on the geography in this region The authors are grateful to two anonymous reviewers for their critical reading of the manuscript and invaluable comments ERS-1/-2 SAR data used in this study were acquired at Syowa Station by the JARE satellite receiving team The European Space Agency retains ownership of the ERS-1/-2 SAR data NCEP atmospheric pressure data were provided by the NOAA-CIRES Climate Diagnostics Center, Colorado, USA, though their Web site at *http://www.cdc noaa gov/* Some figures were drawn using Generic Mapping Tools (Wessel and Smith, 1998)

References

British Antarctic Survey (1998) Antarctic Digital Database, Version 2 0 Manual and bibliography Cambridge, Scientific Committee on Antarctic Research, 74 p

Doi, K , Shibuya, K , Nogi, Y and Ozawa, T (1999) Interferometric SAR images derived from ERS-1/-2 tandem mission data acquired at Syowa Station, Antarctica J Geod Soc Jpn , **45**,

351-354 (in Japanese with English abstract)

Doi K, Ozawa T, Aoki S, Shibuya, K and Oishi, Y (2000) Level 0 CEOS formatted data generating system for SAR data of NIPR Proc Workshop "SAR interferometry and its application" ed by N Fujii Tokyo Earthquake Remote Sensing Frontier Project, in CD-ROM

Goldstein R M, Engelhardt H Kamb, B and Frolich R M (1993) Satellite radar interferometry for monitoring ice sheet motion Application to an Antarctic ice stream Science **262** 1525-1530

Kim, K T, Jezek, K C and Sohn H G (2001) Ice shelf advance and retreat rates along the coast of Queen Maud Land, Antarctica J Geophys Res **106** 7097-7106

Matsumoto, K, Ooe, M Sato T and Segawa J (1995) Ocean tide model obtained from TOPEX/POSEIDON altimetry data J Geophys Res **100**, 25319-25330

Matsumoto, K, Takanezawa, T and Ooe, M (2000) Ocean tide models developed by assimilating TOPEX/POSEIDON altimetry data into hydrodynamical model a global model and a regional model around Japan J Oceanogr, **56** 567-581

National Institute of Polar Research (1988) 1 5,000,000 scaled map of East Queen Maud Land-Enderby Land Tokyo

Orheim, O (1978) Glaciological studies by Landsat imagery of perimeter of Dronning Maud Land Antarctica Norsk Polarinst Skr, **169** 69-80

Ozawa, T Doi K and Shibuya K (1999) Deformation of the Zubchatyy Ice Shelf, Antarctica derived from Synthetic Aperture Radar interferometry J Geod Soc Jpn **45** 165-179 (in Japanese with English abstract)

Rignot E (1996) Tidal motion ice velocity and melt rate of Petermann Gletscher, Greenland measured from radar interferometry J Glaciol, **42** 476-485

Wessel, P and Smith, W H F (1998) New, improved version of the Generic Mapping Tools released EOS Trans AGU, **79**, 579

Zebker, H A and Villasenor J (1992) Decorrelation in interferometric radar echoes IEEE Trans Geosci Remote Sensing **30** 950-959

(Received April 12, 2002, Revised manuscript accepted June 14, 2002)